Solid State Ionics xxx (2010) xxx–xxx

Contents lists available at ScienceDirect

Solid State Ionics

journal homepage: www.elsevier.com/locate/ssi

Comparative study of $NiSb_2$ and $FeSb_2$ as negative electrodes for Li-ion batteries

C. Villevieille, C.M. Ionica-Bousquet, B. Fraisse, D. Zitoun, M. Womes, J.C. Jumas, L. Monconduit *

Institut Charles Gerhardt Montpellier-UMR 5253 CNRS-UM2-ENSCM-UM1, Agrégats, Interfaces et Matériaux pour l'Energie, CC 1502, Place Eugène Bataillon, 34095 Montpellier, France

ARTICLE INFO

Article history:
Received 31 August 2009
Received in revised form 2 April 2010
Accepted 26 April 2010
Available online xxxx

Keywords:
Conversion reaction
Negative electrode
Lithium-ion batteries
Iron di-antimonide
Ternary lithiated phase
Electrochemical process

ABSTRACT

Crystalline $FeSb_2$ powder prepared by ceramic route is examined as negative electrodes for lithium-ion batteries. The complete reaction mechanism of $FeSb_2$ is investigated by ^{121}Sb and ^{57}Fe Mössbauer spectroscopy as well as magnetic measurements and the results are correlated with a previous *in situ* XRD characterization. On the first discharge the reaction with Li proceeds through a biphasic process transforming $FeSb_2$ into a new $Li_xFe_ySb_2$ phase, and this ternary phase is then converted into *fcc* Li_3Sb and metallic Fe nanoparticles. The combination of Mössbauer spectroscopy and magnetic analyses leads i) to a better understanding of the $FeSb_2 \rightarrow$ ternary phase reaction and concomitantly allowed ii) to specify the stoichiometry of the new ternary phase. On charge, the extrusion of lithium includes the back conversion of the Li_3Sb/Fe mixture into both $Li_4Fe_{0.5}Sb_2$ and metallic Sb, which are the main active species for the following cycles, responsible for the poor cycling life of the $FeSb_2$ electrode. The nature of these resulting products is quite different from that previously observed for the isotype $NiSb_2$ electrode which is characterized by a highly reversible mechanism.

1. Introduction

Many efforts have been expended in the last decade to improve Li-ion batteries. Although significant improvements in the performance were obtained (increase in energy density and rate capability), the exploration of new materials and the understanding of their electrochemical mechanisms are still primary to better control the electrode properties and the battery performances. Over the past few years, some Sb-based intermetallic compounds, such as InSb [1], $CoSb_3$ [2–4] or Cu_2Sb [5,6] have been intensively investigated as negative electrodes for lithium-ion batteries, showing higher capacities than the commercialised carbon material. Unfortunately, they suffered from an important capacity fading. A previous study of $NiSb_2$ as negative electrode [7] demonstrated the great interest to study the MSb_2 antimonides with an FeS_2 marcasite-type structure (where M is a transition metal (Fe, Co, Ni))[8,9]. In this field Xie et al. described succinctly the electrochemical behaviour of $FeSb_2$, obtained by mechanical levitation reaction and no mechanism was proposed [10]. In a more recent paper we demonstrated through a combined electrochemical and *in situ* XRD study that the electrochemical mechanism of $FeSb_2$/Li occurs in two steps on the first discharge (the galvanostatic curve of $FeSb_2$/Li cell is reminded on Fig. 1) [11]. *in situ* XRD analysis gave the following results: i) during the plateau at 0.62 V (4Li) a continuous decrease in the intensity of the main $FeSb_2$ Bragg peaks to the expense of a new set of Bragg peaks not ascribable to any known phase; ii) along the second plateau at 0.4 V (1.5Li), XRD shows a continuous shift of this new set of broad peaks to smaller angles; and iii) at the end of the discharge the formation of the high temperature cubic Li_3Sb phase ($a = 6.572$ Å, Fm3m). From these XRD *in situ* data we deduced that the intermediate unknown ternary phase was isotype to the face-centered-cubic Li_3Sb phase and has a composition close to "Li_4FeSb_2".

In order to get deeper insight in the mechanism of the $FeSb_2$/Li cell during the cycling and to better describe this new intermediate phase we decided to investigate the discharge/charge cycle by ^{121}Sb and ^{57}Fe Mössbauer spectroscopy and magnetic measurements. Both characterizations give useful information both on the nature of the electrochemically formed phases and on the changes of the electronic states during the reduction/oxidation processes. Finally the proposed electrochemical behaviour of $FeSb_2$ will be compared with the mechanism previously elucidated for its isotype $NiSb_2$ [7,12] and the differences will be discussed.

2. Experimental aspects

2.1. Synthesis procedure

$FeSb_2$ sample was prepared by direct synthesis from the pure elements: iron (Alfa Aesar, 350 mesh, 99.9%) and antimony (Alfa Aesar, 350 mesh, 99%) in silica tubes sealed under vacuum. After annealing for 7 days at 720 °C using a ramp of 1 °C/min, the tube was air-quenched.

2.2. Electrochemical tests

The setup used for the electrochemical characterization is described elsewhere [11].

* Corresponding author.
E-mail address: laure.monconduit@univ-montp2.fr (L. Monconduit).

0167-2738/$ – see front matter © 2010 Elsevier B.V. All rights reserved.
doi:10.1016/j.ssi.2010.04.029

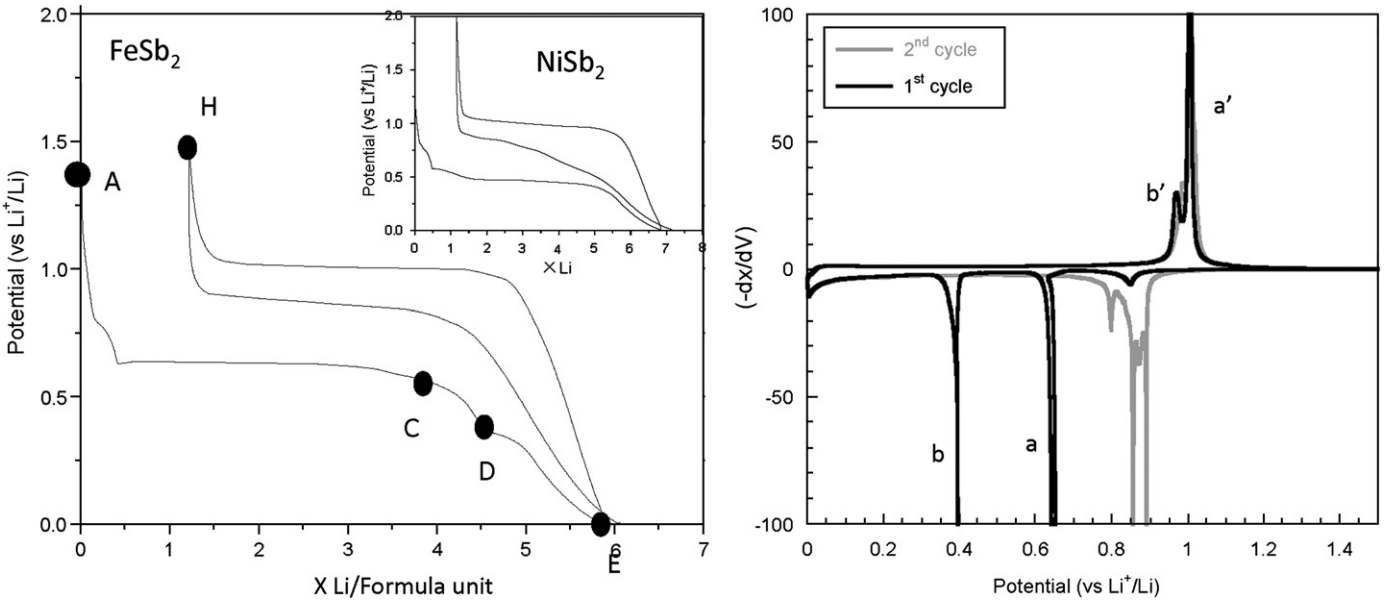

Fig. 1. Potential plotted versus composition for a $FeSb_2$/Li cell cycled between 1.5 and 0 V at C/20. The derivative $-dx/dV$ plot is shown for the first cycles. Points A to H mark the samples which were analysed by Mössbauer spectroscopy and magnetic measurements. For comparison reasons the inset presents the galvanostatic curve for a $NiSb_2$/Li cell cycled between 2 and 0 V at C/20.

2.3. Mossbauer spectroscopy

^{121}Sb Mössbauer measurements were performed using a ^{121m}Sn in $BaSnO_3$ source of nominal activity 0.5 mCi on an EG & *G* constant acceleration spectrometer in transmission mode. During the measurements, both source and absorbers were simultaneously cooled down to 4.2 K. The zero isomer shift was defined from the spectrum of InSb at 4.2 K ($\sigma = -8.72(4)$ mm s^{-1} relative to $Ba^{121m}SnO_3$). ^{57}Fe Mössbauer measurements were carried out at room temperature, using a ^{57}Co(Rh) source with a nominal activity of 370 MBq (=10 mCi). ^{57}Fe shifts are given with respect to the centre of the six-line-spectrum of the α-Fe foil.

2.4. Magnetic measurements

Magnetic properties were measured on a Superconducting Quantum Interference Design (SQUID) magnetometer MPMS XL7 between 2 and 300 K in magnetic fields between 0 and 5 T. The temperature dependent susceptibility was measured using a DC procedure. Measurements on electrode materials were carried out *ex situ* after extraction of the electrode material from the Swagelok cell.

3. Results and discussions

The phase purity of the $FeSb_2$ intermetallic was checked by X-ray diffraction. The Bragg peaks could all be indexed on the basis of an orthorhombic marcasite cell with the following refined lattice parameters: $a = 5.829(2)$ Å; $b = 6.535(1)$ Å; $c = 3.197(1)$ Å in good agreement with the values given in the literature [13].

As mentioned in the introduction the mechanism was previously proposed for the first discharge as following [11]:

$$0.62\text{V} \quad FeSb_2 + 4\ Li \rightarrow \text{“}Li_4Fe_ySb_2\text{”} \tag{1}$$

$$0.4\text{V} \quad \text{“}Li_4Fe_ySb_2\text{”} + 2\ Li \rightarrow 2Li_3Sb + yFe^0 \tag{2}$$

On charge, 4.5 Li are removed corresponding to a reversible capacity of 420 mAh g^{-1} (or 3500 mAh cm^{-3}) (Fig. 1). A double process appears between 1.1 and 0.9V (Fig. 1, a′ and b′ on the derivative curve). During the second discharge, we observe a single voltage plateau centered at 0.75 V.

On Fig. 2 XRD *in situ* analysis performed during the first charge shows: i) a shift of the Li_3Sb fcc Bragg peaks to the upper angles which means the restructuration of the “$Li_4Fe_ySb_2$” phase and then ii) a decrease of the peak intensity of this new phase to the benefit of another one which seems to be amorphous. During the second discharge (not shown here) XRD shows the reappearance of Li_3Sb.

Mössbauer spectroscopy and magnetic measurements were carried out in order to identify the nature of this new phase reversibly formed on discharge and charge, and to elucidate the electrochemical reaction mechanism. Fig. 3a shows the evolution of the ^{121}Sb Mössbauer spectrum recorded at different depths of the discharge (points A to E) and at the end of the charge process (point H). All the spectra have been accurately analyzed to obtain the hyperfine parameters, i.e. isomer shift (δ), quadrupole splitting (eQVzz), linewidth (Γ_a) and contribution of each component. The corresponding refined hyperfine parameters are reported in Table 1. The ^{121}Sb Mössbauer spectrum of $FeSb_2$ (Fig. 3a, point A) was fitted with two components. The isomer shift of the first of $\delta = -1.23$ mm s^{-1} is characteristic of intermetallic compounds and was assigned to $FeSb_2$. [13,14] The second component $\delta = 8.83$ mm s^{-1} was assigned to Sb_2O_5 formed as an impurity during the synthesis process [15]. After the first discharge plateau at 0.62 V, the Mössbauer spectrum obtained for $x \approx 4$ Li (point C) shows the appearance of a new component attributed to the formation of a new phase denoted hereafter “X phase” ($\delta \sim -2.42$ mm s^{-1}, eQVzz = 9.96 mm s^{-1}, 75% relative contribution), with a residual presence of the $FeSb_2$ (13%). Comparison with data from literature allowed no identification of this new “X phase”. As illustrated in Fig. 3a, point D (discharge down to 0.28 V), the contribution of the multiplet of the “X phase” decreases to 25% and that of $FeSb_2$ disappears in favour of a new component assigned to cubic Li_3Sb ($\delta \sim -1.07$ mm s^{-1}, eQVzz = 0 mm s^{-1}, 60% relative contribution) [8]. At the end of the first discharge the Mössbauer spectrum mainly reflects Li_3Sb and Sb_2O_5 as an impurity. On full charge at 1.5 V ($x = 1.2$ Li, point H) the Mössbauer spectrum shows a majority of metallic Sb ($\delta \sim -3.28$ mm s^{-1}, eQVzz = 3.13 mm s^{-1}, 56%) and also unreacted Li_3Sb (12% relative contribution) and “X phase” (22% relative contribution). The hyperfine parameters and relative contribution of the “X phase” are identical

Please cite this article as: C. Villevieille, et al., Comparative study of $NiSb_2$ and $FeSb_2$ as negative electrodes for Li-ion batteries, Solid State Ion. (2010), doi:10.1016/j.ssi.2010.04.029

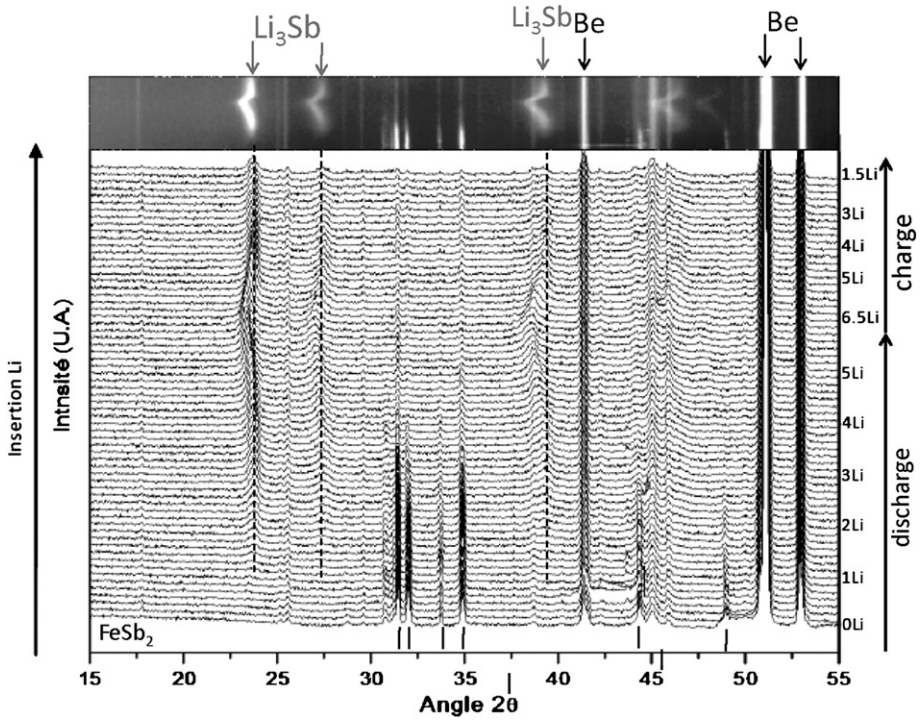

Fig. 2. XRD *in situ* for the first cycle of the $FeSb_2$/Li cell

to those obtained for the electrode discharged at 0.28 V (point D). The formation of metallic Sb (undetected by XRD) as the main component at the end of the first charge was already observed for Mn–Sb/Li cell [9]. The sample discharged at 0.28 V (point D) corresponding to the end of the first biphasic plateau (Fig. 3b), was also analyzed by ^{57}Fe Mössbauer spectroscopy. In this spectrum three different environments for Fe were identified, characterized by two doublets and one singlet. The doublet ($\delta \sim 0.54$ mm s^{-1}, $\Delta Eq = 0.18$ mm s^{-1}) could not be identified on the basis of the available literature data and was assigned to Fe in the "X phase" (36% relative contribution). The two other components (64%), i.e. the singlet and the doublet, centered at about 0 mm s^{-1} were assigned to two types of iron, 31% core Fe and 33% surface Fe extruded during the (Reaction (1)) electrochemical process. That means that the X phase is less rich in Fe than initially thought. It is noticeable i) that the $FeSb_2$ pristine material [16] was completely consumed during this first process (Reaction (1)) and ii) that the ratio "X phase"/Fe close to 0.36/0.64 is well consistent with the ratio 0.3/0.7 found for "X phase"/Li_3Sb by ^{121}Sb Mössbauer spectroscopy at point D, meaning that Reaction (2) has started at 0.28V.

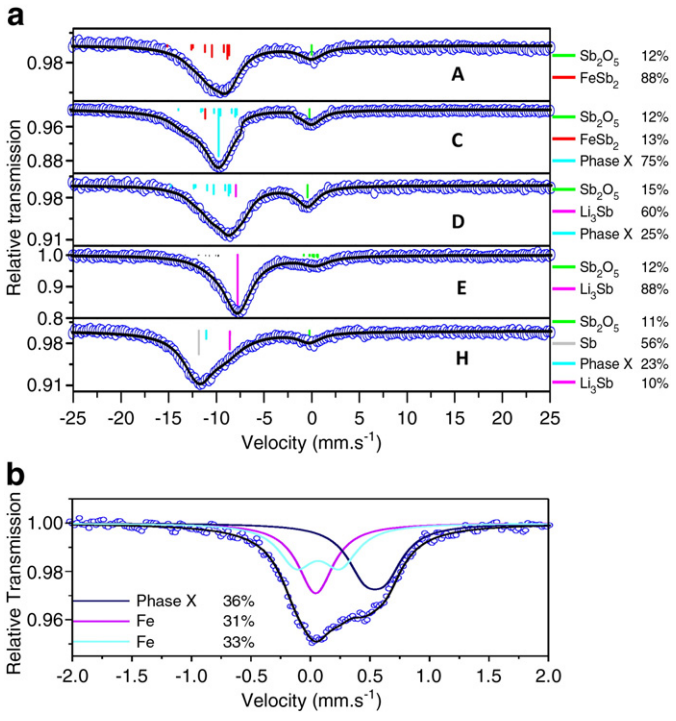

Fig. 3. a)^{121}Sb Mössbauer spectra of $FeSb_2$ during first discharge (A to E points) and at the end of the charge (H point); b) ^{57}Fe Mössbauer spectrum of $FeSb_2$ electrode (D point) recorded at room temperature.

Measurements of the saturation magnetization at 2 K were carried out for the quantitative evaluation of metallic iron. The field dependence of the magnetization measured at 2 K, at different depths of lithiation of the $FeSb_2$ electrode material is shown in Fig. 4. The saturation magnetization Ms of the starting material $FeSb_2$ at 2 K is 1.4 A m^2/kg$_{Fe}$. The reaction of $FeSb_2$ with lithium during the first discharge leads to a progressive growth of the saturation magnetization, reaching 112 A.m^2/kg$_{Fe}$ at the end of the first potential plateau (point C). This result, compared to the saturation magnetization of bulk metallic iron (210Am^2/kg), correlated with the absence of Li_3Sb at this point C (previously shown by ^{121}Sb spectroscopy), demonstrates that more than 50% of Fe present in the starting $FeSb_2$ has been extruded during process (1). The saturation magnetization reaches a 202 A m^2/kg$_{Fe}$ at full discharge (point E) which is close that of bulk metallic Fe. It indicates the transformation of 96% of the starting material into metallic iron. During the next charge, from 0 V to 1.1 V the magnetization decreased strongly and reaches 101 A m^2/kg$_{Fe}$ at 1.1 V. This value is close to that obtained during the discharge at point C point and can be assigned to the reformation of the ternary "X phase". This remark is consistent with the results obtained by Mössbauer Spectroscopy and *in situ* XRD. Further charge up to 1.5 V (point H) does not produce significant changes on the magnetization value indicating that no further reaction involving Fe atoms takes place during this delithiation process.

Please cite this article as: C. Villevieille, et al., Comparative study of $NiSb_2$ and $FeSb_2$ as negative electrodes for Li-ion batteries, Solid State Ion. (2010), doi:10.1016/j.ssi.2010.04.029

Table 1
^{121}Sb Mössbauer parameters obtained at 4.2 K for samples A to H (see discharge and charge curves of Fig. 1). Isomer shift δ relative to InSb (−8.72 mm/s relative to the source $Ba^{121m}SnO_3$ source) (on Fig. 3a, δ are relative to the source), eQV_{zz}: quadrupole splitting, $\Gamma = \Gamma^a$, absorber linewidth (source linewidth $\Gamma_s = 1.45$ mm/s), C: relative contribution. ^{57}Fe parameters obtained at room temperature for sample D; δ: isomer shift relative to α-Fe, ΔEq: quadrupole splitting; (2) $\Gamma = \Gamma_s + \Gamma_a$ total linewidth; C: relative contribution.

Sample	Li in $FeSb_2$	δ (mm s^{-1})	eQVzz (mm s^{-1})	Γ (mm s^{-1})	C (%)	Identification
1st discharge — ^{121}Sb						
A	0	−1.23 (2)	13.6 (2)	1.59 (3)	88	$FeSb_2$
	(2.84 V)	8.83 (1)	−3.80 (1)	1.59 (3)	12	Sb_2O_5
C	4	−1.16 (2)	13.45 (2)	1.60 (5)	13	$FeSb_2$
	(0.57 V)	−2.42 (2)	9.96 (2)	1.60 (5)	75	Phase X
		8.85(3)	−3.68(2)	1.60 (5)	12	Sb_2O_5
D	4.5	−2.36 (4)	10.04 (3)	1.52 (3)	25	Phase X
	(0.28 V)	1.07 (1)	–	1.52 (3)	60	Li_3Sb
		8.72(3)	−3.62(2)	1.52 (3)	15	Sb_2O_5
E	6.5	1.04 (2)	–	1.32 (6)	88	Li_3Sb
	(0.0 V)	8.72 (3)	−3.58 (2)	1.32 (6)	12	Sb_2O_5
1st charge — ^{121}Sb						
H	1.2	−2.39 (4)	10.05(4)	1.70 (4)	22	Phase X
	(1.5 V)	−3.28 (1)	3.13(2)	1.64 (4)	56	Sb
		1.08 (2)	–	1.52 (4)	12	Li_3Sb
		8.93 (3)	−3.64	1.58(4)	10	Sb_2O_5
1st discharge — ^{57}Fe						
D	4.5	0.54 (1)	0.18 (1)	0.36 (1)	36	Phase X
	(0.28 V)	0.06 (1)	0.37 (1)	0.36 (1)	33	Fe
		0.04 (1)	–	0.36 (1)	31	Fe

Starting from our previous mechanism investigation of the $FeSb_2$–Li system by *in situ* XRD we proposed the new ternary phase "X phase" to be isotype of *fcc* Li_3Sb with a nominal composition close to the Li_4FeSb_2. It can be noted that Li–TM–Sb ternary phases, with TM a transition metal, are very rare. Only the *fcc* Li_2CuSb [5] phase is reported in the literature with a cell parameter (a=6.27Å) close to that observed for this X phase. The present characterization by ^{57}Fe Mössbauer Spectroscopy and SQUID measurements allow us to conclude that half of the iron particles were extruded during the first biphasic plateau corresponding to a biphasic reaction $FeSb_2 \rightarrow Li_4Fe_ySb_2$, where $y \approx 0.5$. Afterward the discharge proceeds through the transformation of $Li_4Fe_ySb_2$ to *fcc* Li_3Sb and Fe. During the charge process the correlation of all these results allows us to conclude that the reaction mechanism is more complex with a competition between two processes: firstly the reformation of the ternary $Li_4Fe_{0.5}Sb_2$ phase by the reaction of Li_3Sb with Fe particles and secondly the delithiation of Li_3Sb to form amorphous Sb as main component.

As already mentioned the electrochemical mechanism of $NiSb_2$ phase (Fig. 1 inset) was previously elucidated in our group and we found it interesting to compare the two reaction mechanisms. Table 2 summarizes the two reaction mechanisms. Although both di-antimonides are isostructural, their electrochemical behaviour is quite different. Like in the case of $FeSb_2$, the discharge reaction of $NiSb_2$ proceeds in two steps. After a first process of topotactic insertion of less than 1 Li^+ in $NiSb_2$, associated with a limited volume expansion (<1%), a biphasic reaction takes place, converting the Li_xNiSb_2 phase (x<1) to the ($2Li_3Sb + Ni°$) composite electrode. The

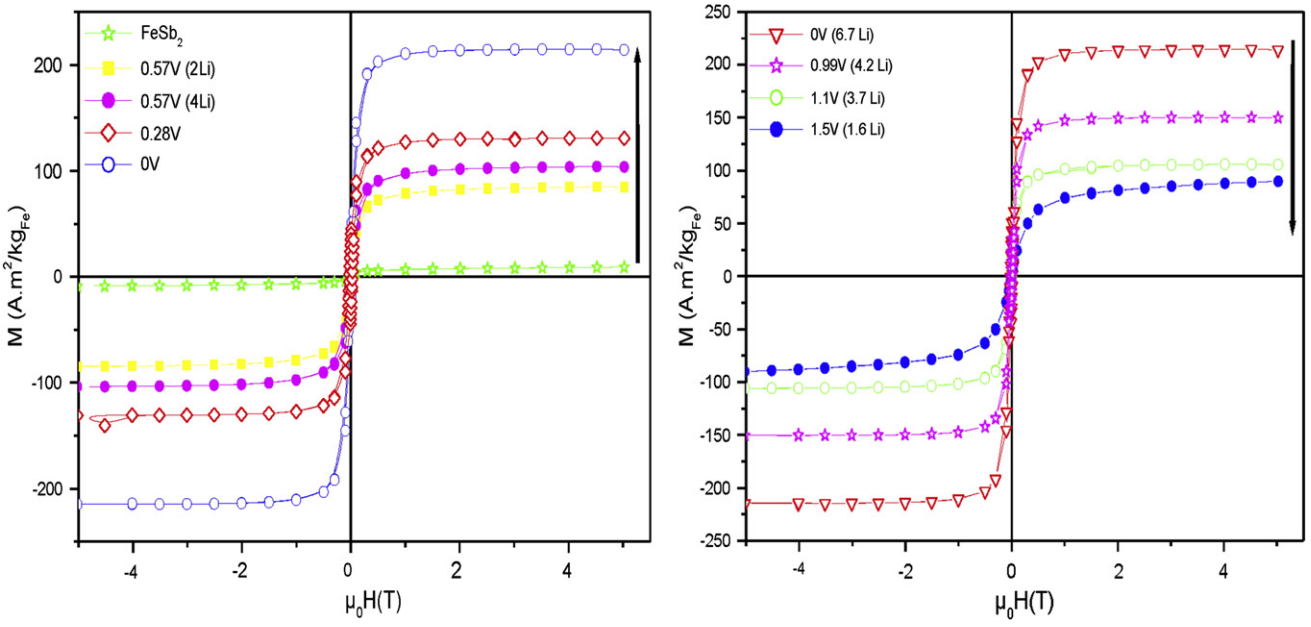

Fig. 4. Field dependence at 2 K of the magnetization of $FeSb_2$ electrode at various depths of discharge/charge.

Please cite this article as: C. Villevieille, et al., Comparative study of $NiSb_2$ and $FeSb_2$ as negative electrodes for Li-ion batteries, Solid State Ion. (2010), doi:10.1016/j.ssi.2010.04.029

Table 2
Summary of the electrochemical reaction mechanisms for $FeSb_2$ and $NiSb_2$ electrode materials.

$NiSb_2$		$FeSb_2$	
1st discharge			
Potential/Li	Reactions	Potential/Li	Reactions
0.5Li	SEI	0.5Li	SEI
0.5-1Li	Solid solution $NiSb_2 \rightarrow Li_xNiSb_2$	0.5Li–4 Li	Transformation/extrusion $FeSb_2 \rightarrow Li_4Fe_{0.5}Sb_2 + 0.5\ Fe^\circ$
1Li–7Li	Conversion reaction $Li_xNiSb_2 \rightarrow 2Li_3Sb + Ni^\circ$	4Li–6Li	Displacement $Li_4Fe_{0.5}Sb_2 \rightarrow 2Li_3Sb + 0.5\ Fe^\circ$
1st charge			
7Li–3.5Li	Conversion of Li_3Sb/Ni° into $NiSb_2$ high pressure form	6Li–3Li	Back conversion $2Li_3Sb + 0.5\ Fe^\circ \rightarrow Li_xFe_ySb_2$
3.5Li–1.2Li	Conversion of Li_3Sb into Sb	3Li–1.3Li	Conversion of $Li_3Sb \rightarrow Sb$ (XRD amorphous)

further discharges lead also to the Li_3Sb matrix and Ni metallic particle formation. Although this second step of the discharge is quite similar to that observed in the case of $FeSb_2$, the charge process is very different. The lithium extraction from the composite Li_3Sb/Ni discharged electrode takes place in two steps leading to the formation of high pressure HP–$NiSb_{2-\varepsilon}$ as the predominant phase and of metallic Sb formation [7].

4. Conclusion

The present work has focused on: (i) the analysis of the mechanisms which occur during the first discharge/charge reactions of the $FeSb_2$/Li cell; (ii) the structural changes induced by the reduction/oxidation processes; and (iii) the identification of the resulting products.

The *in situ* XRD results give an incomplete picture of the processes that occur in the $FeSb_2$ electrode. Additional ^{121}Sb and ^{57}Fe Mössbauer Spectroscopy characterization correlated with magnetic measurements gives access to a better understanding of the reactions which occur upon cycling. Two biphasic reactions were observed for the $FeSb_2$ electrode. First a new ternary $Li_4Fe_ySb_2$ phase ($y \approx 0.5$) is obtained through a biphasic process accompanied by Fe extrusion. It is followed by a Li/Fe substitution reaction leading to Li_3Sb and Fe nanoparticles.

$$FeSb_2 + 4\ Li \rightarrow Li_4Fe_{0.5}Sb_2 + 0.5\ Fe^0 \quad (1')$$

$$Li_4Fe_{0.5}Sb_2 + 2\ Li \rightarrow 2Li_3Sb + 0.5Fe^0 \quad (2')$$

During the charge process, this composite is transformed into the ternary $Li_4Fe_ySb_2$ phase including back reaction with Fe nanoparticles. Furthermore, a lithium extrusion from the remaining Li_3Sb took place to form amorphous Sb. The ternary phase/Sb mixture is the active material responsible for the next cycles of the cell. In the di-antimonide family of intermetallics, different electrochemical processes take place depending on the nature of the transition metal. Finally $FeSb_2$ and $NiSb_2$ compounds show a two steps mechanism occurring upon the first discharge and leading to *fcc* Li_3Sb and metallic nanoparticles. Different intermediates, which are ternary lithiated phases never described in the literature, are formed. Moreover, the resulting products of the following charge process are different and in the case of $NiSb_2$ the stabilization of the closer packed HP–$NiSb_{2-\varepsilon}$ structure seems to be favorable for improving the electrochemical performances in terms of reversible capacities and cycle life, as compared to $FeSb_2$.

Additionally electronic band calculations are in progress to better understand and explain the role of the transition metal and its influence on the electrochemical mechanism.

References

[1] K.C. Hewitt, L.Y. Beaulieu, J.R. Dahn, J. of Electrochemical Soc. 148 (5) (2001) A402.
[2] J. Xie, X.B. Zhao, G.S. Cao, M.J. Zhao, S.F. Su, J. of Power Sources 140 (2005) 350.
[3] J. Xie, X.B. Zhao, G.S. Cao, S.F. Su, J. of Electrochemical Soc. 152 (3) (2005) A601.
[4] J.M. Tarascon, M. Morcrette, L. Dupont, Y. Chabre, C. Payen, D. Larcher, V. Pralong, J. Electrochem. Soc 150 (6) (2003) A732.
[5] M. Morcrette, D. Larcher, J.M. Tarascon, K. Edström, J.T. Vaughey, M.M. Thackeray, Electrochimica Acta 52 (2007) 5339.
[6] L.M.L. Fransson, J.T. Vaughey, R. Benedek, K. Edström, J.O. Thomas, M.M. Thackeray, Electrochem. Commun. 3 (2001) 317.
[7] C. Villevieille, C.-M. Ionica-Bousquet, B. Ducourant, J.-C. Jumas, L. Monconduit, J. of Power Sources 172 (2007) 388.
[8] L. Aldon, A. Garcia, J. Olivier-Fourcade, J.-C. Jumas, F.J. Fernández-Madrigal, P. Lavela, C.P. Vicente, J.L. Tirado, J. of Power Sources 119–121 (2003) 585.
[9] C.M. Ionica, P.-E. Lippens, J. Olivier-Fourcade, J.-C. Jumas, J. of Power. Sources 146 (2005) 478.
[10] J. Xie, X.B. Zhao, G.S. Cao, M.J. Zhao, Y.D. Zhong, L.Z. Deng, Mat. Let. 57 (2003) 4673.
[11] C. Villevieille, B. Fraisse, M. Womes, J.C. Jumas, L. Monconduit, J. of Power. Sources 189 (1) (2009) 324.
[12] C. Villevieille, C.M. Ionica-Bousquet, J.-C. Jumas, L. Monconduit, Hyperfine Interactions 187 (2008) 1157.
[13] J.D. Donalson, A. Kjekshus, D.G. Nicholson, M.J. Tricker, Acta Chem. Scand. 26 (1972) 3215.
[14] A.A. Temperley, H.W. Lefevre, J. of Phys. Chem. Solids 27 (1966) 85.
[15] L. Bowen, J. Inorg. Nucl. 33 (1971) 953.
[16] J. Steger, E. Kostiner, J. Solid State Chem. 5 (1972) 131.

Please cite this article as: C. Villevieille, et al., Comparative study of $NiSb_2$ and $FeSb_2$ as negative electrodes for Li-ion batteries, Solid State Ion. (2010), doi:10.1016/j.ssi.2010.04.029